

## REMOVAL OF ACETAMINOPHEN BY USING ELECTROSPUN PAN/SAGO LIGNIN-BASED ACTIVATED CARBON NANOFIBERS

Dzaidatu Aqmal Ramlee<sup>1</sup>, Nurul Aida Nordin<sup>1</sup>, Norizah Abdul Rahman<sup>1,2\*</sup> and Hasliza Bahruji<sup>3</sup>

<sup>1</sup>Department of Chemistry, Faculty of Science, Universiti Putra Malaysia, Serdang 43400, Selangor, Malaysia

<sup>2</sup>Nanomaterials Processing and Technology Laboratory, Institute of Nanoscience and Nanotechnology, Universiti Putra Malaysia, UPM, Serdang 43400, Selangor, Malaysia.

<sup>3</sup>Centre of Advanced Materials and Energy Science, University Brunei Darussalam, Jalan Tungku Link, Gadong BE 1410, Brunei Darussalam

\*Corresponding author: a\_norizah@upm.edu.my

Received: 27 October 2023; Accepted: 2 June 2024; Published: 29 December 2024

### Abstract

Pharmaceutical compounds have been identified as contaminants of emerging concern (CEC) in wastewater because of their potential hazards to humans and aquatic organisms. One of the emerging pollutants is acetaminophen, commonly known as paracetamol, which is frequently consumed worldwide as an analgesic, painkiller, and antipyretic compound. Various methods have been developed to remove acetaminophen from wastewater and water bodies, with adsorption being the cheapest and easiest method. This study prepared activated carbon nanofibers (ACNFs) via consecutive electrospinning, stabilization, carbonization, and activation methods for removing acetaminophen from aqueous solution. Fibers with larger diameters were obtained at higher PAN/sago lignin (PAN/SL) ratios during electrospinning. Uniform bead-free nanofibers produced with 20 wt% lignin were stabilized and carbonized to produce carbon nanofibers (CNFs). ACNFs activated via KOH displayed increased oxygen-containing functional groups that efficiently removed acetaminophen from the aqueous solution. SEM images showed that the diameter of the nanofibers decreased after heat treatment. The adsorption of acetaminophen on ACNFs was evaluated based on four parameters: the effect of the initial concentration of acetaminophen, contact time, adsorbent dosage, and pH of the solution. The adsorption behavior of the PAN/SL ACNFs showed no significant changes at pH 3 to 9. The optimum parameters for acetaminophen were an initial concentration of 25 mg/L, an adsorbent dose of 0.1 g, and a reaction time of 60 min. The results showed that the ACNF adsorption capacity increased to 52 mg/g, indicating that PAN/SL ACNFs are good adsorbents for acetaminophen in aqueous solution.

**Keywords:** carbon nanofibers, activated carbon, electrospinning, sago lignin, PAN

### Abstrak

Sebatian farmaseutikal telah dikenal pasti sebagai bahan cemar yang menjadi kebimbangan baharu (CEC) dalam air sisa kerana potensi bahayanya kepada manusia dan organisma akuatik. Salah satu bahan cemar yang sedang muncul ialah asetaminofen, yang lebih dikenali sebagai parasetamol, yang kerap digunakan di seluruh dunia sebagai sebatian analgesik, penahan sakit, dan antipiretik. Pelbagai kaedah telah dibangunkan untuk menghapuskan asetaminofen daripada air sisa dan badan air, dengan penjerapan menjadi kaedah yang paling murah dan mudah. Kajian ini menyediakan nanoserat karbon teraktif (ACNF) melalui kaedah putaranelektro berturutan, penstabilan, pengkarbonan, dan pengaktifan untuk menyingkirkan asetaminofen daripada larutan akueus. Serat dengan diameter lebih besar diperolehi pada nisbah poliakrilonitril/lignin sago (PAN/SL) yang lebih tinggi semasa putaranelektro. Nanoserat seragam tanpa manik yang dihasilkan dengan 20% berat lignin telah distabilkan dan dikarbonkan untuk menghasilkan nanoserat karbon (CNF). ACNF yang diaktifkan menggunakan KOH menunjukkan peningkatan kumpulan berfungsi

yang mengandung oksigen, yang secara berkesan menyingkirkan asetaminofen daripada larutan akueus. Imej SEM menunjukkan diameter nanoserat berkurang selepas rawatan haba. Penjerapan asetaminofen pada ACNF dinilai berdasarkan empat parameter: kesan kepekatan awal asetaminofen, masa sentuhan, dos penjerap, dan pH larutan. Tingkah laku penjerapan ACNF PAN/SL menunjukkan tiada perubahan ketara pada pH 3 hingga 9. Parameter optimum untuk asetaminofen ialah kepekatan awal 25 mg/L, dos penjerap 0.1g, dan masa tindak balas selama 60 minit. Hasil kajian menunjukkan kapasiti penjerapan ACNF meningkat kepada 52 mg/g, menandakan bahawa ACNF PAN/SL merupakan penjerap yang baik untuk asetaminofen dalam larutan akueus.

**Kata kunci:** nanoserat karbon, karbon teraktif, putaranelektro, lignin sago, PAN

### Introduction

Global economic growth has promoted the development of functional chemical products required for human, manufacturing industry, and veterinary health. Disposal of these compounds, such as water, air, and soil, affects the environment. Previous studies estimated that globally, 380 billion m<sup>3</sup> (m<sup>3</sup> = 1000 L) of wastewater is produced annually [1]. Consequently, water pollution has become a severe problem in countries with poor water treatment systems [2]. Acetaminophen, commonly known as paracetamol, is a pain reliever and an antipyretic drug widely used and considered the best-selling drug worldwide because of its accessibility to the public without the need for consultation [3]. Its presence in water resources has been associated with liver damage, infertility, and feminization in aquatic species [4]. It is also one of the most commonly detected pharmaceutical compounds in aquatic environments because of its high solubility in water [5]. Pharmaceutical compound effluents should be properly treated before they are safely discharged into aquatic ecosystems [6]. To date, numerous methods have been developed to remove pharmaceutical compounds from water effluents. However, adsorption is preferred because of its simplicity, low cost, and high efficiency [7]. In recent years, carbon-based materials, such as activated carbon nanofibers (ACNF), granular activated carbon, and carbon nanotubes, have been efficient adsorbents for water treatment [8-10]. Generally, a highly developed specific surface area, porosity, and interconnected open pore structure are necessary for adsorbent materials to achieve high adsorption capacity [11-12]. Therefore, ACNFs have been widely adopted as adsorbents for water treatment. Polyacrylonitrile (PAN) is a petroleum-based material extensively used as a precursor to produce carbon nanofibers with excellent mechanical properties, good electrospinnability, and a high carbon yield [13, 14]. Alternatively, using lignin as a precursor for carbon nanofibers (CNF) has gained

significant interest owing to its low cost and renewable resources [15, 16].

Lignin is an amorphous three-dimensional polymer composed of three types of methoxylated phenylpropene monomeric units. Lignin is one of the best substitute materials for producing carbon nanofibers because it is a carbon-rich component of biomass and one of the main sources of renewable aromatic compounds [17]. Pulp and paper are among the largest industrial commodities in the world, contributing to the production of lignin biopolymers [18]. Polymer nanofiber fabrication often employs the electrospinning technique owing to its simple procedure to form small fibers, which is crucial for controlling the morphology of CNFs. The electrospinning technique transforms the lignin solution into fibers with diameters ranging from the submicron to the nanoscale. Research has progressively reported the use of electrospinning for the fabrication of lignin-based carbon fibers [19]. Lignin-based carbon nanofibers exhibit unique properties that can be used to develop value-added materials at low production costs. The "green" carbon adsorbent has potential applications in water filtration. This study prepared PAN/sago Lignin (SL)-based ACNFs via consecutive electrospinning, thermal treatment, and chemical activation. Lignin was isolated from sago waste and blended with PAN to produce ACNFs. As reported previously by our group, sago lignin can be homogeneously blended with PAN [8]. The prepared PAN/SL ACNFs were then used as adsorbents to remove acetaminophen from the aqueous solutions.

### Materials and Methods

#### Materials

Sago waste was obtained from the Malaysian Nuclear Agency Bangi Complex. Benzene, 95% ethanol, polyacrylonitrile (PAN), Mw 150000, dimethylformamide (DMF), potassium hydroxide

(KOH), hydrochloric acid (HCl) and acetaminophen were purchased from Sigma-Aldrich.

### Preparation of PAN/SL nanofibers and PAN/SL carbon nanofibers (CNFs)

Sago lignin was isolated from sago waste using a previously reported method [20] with slight modifications. The sago waste was treated with sulfuric acid (H<sub>2</sub>SO<sub>4</sub>) in a water bath for 2 h. The mixture was transferred to a flask, 300 mL of distilled water was added, and it was then refluxed for 3 h. Sago lignin was filtered, washed with distilled water, and dried at room temperature. To prepare the PAN/SL nanofibers, PAN was first dissolved in DMF to prepare a 7.5% (wt/v) PAN solution. Sago lignin was then blended with a 7.5% (wt/v) PAN solution, in which the ratio of PAN: sago lignin (wt/wt) was varied at different wt%: 9:1, 8:2, 7:3, 6:4, and 5:5. For the electrospinning process, the polymer solution was filled in a 5 mL syringe attached to 0.8 mm needle diameter. The distance from the collector to the needle tip was 10 cm, the voltage applied was 18 kV, and the solution was electrospun at a 2 mL h<sup>-1</sup> flow rate. To prepare PAN/SL carbon nanofibers, PAN/SL nanofibers were thermally stabilized in a tube furnace at 235 °C for 1 h under an air atmosphere at a heating rate of 1 °C min<sup>-1</sup>. The nanofibers were further carbonized at higher temperatures up to 1000 °C for 1 h under a nitrogen atmosphere at a heating rate of 10 °C min<sup>-1</sup>. The resulting carbon nanofibers were denoted as PAN/SL CNFs.

### Preparation of PAN/SL activated carbon nanofibers (ACNFs)

PAN/SL CNFs were activated into PAN/SL activated carbon nanofibers using potassium hydroxide (KOH) according to the method proposed by [21], with slight modifications. 1.0 g of CNF was mixed with 4.0 g of KOH solution containing 10.0 g of distilled water and sonicated in a water bath at 60 °C. The mixture was then dried at 100 °C before activating for 2 h at 900 °C under a nitrogen flow of 200 mL min<sup>-1</sup>. The heating rate used for this activation was 10 °C min<sup>-1</sup>. The sample was washed with 5 wt% HCl, followed by deionized water. The activated carbon nanofibers were then dried overnight at 100 °C. The activated carbon nanofibers were denoted as PAN/SL ACNFs.

### Batch adsorption of acetaminophen

The adsorption study was conducted by contacting 25 mg of CNFs and ACNFs with 25, 50, 75, and 100 mg/L of the acetaminophen solution. The adsorption study was optimized to obtain the maximum adsorption capacity,  $q_m$ . The adsorption performance of acetaminophen on the ACNFs was studied using four parameters: contact time (s), adsorbent dosage (mg), initial concentration of acetaminophen (mg L<sup>-1</sup>), and pH of the solution. The samples were then shaken at 200 rpm. Samples were withdrawn and filtered at predetermined times. The concentration of the remaining acetaminophen was determined using a UV-Vis spectrophotometer (Model UV9500) at a maximum adsorption wavelength of 242 nm. The percentage removal of acetaminophen (%) and the adsorption capacity (q) were calculated according to Equations (1) and (2), respectively,

$$\text{Removal (\%)} = \frac{C_0 - C_t}{C_0} \times 100 \quad (1)$$

$$\text{Adsorption capacity, } q_m = \frac{C_0 - C_t}{m} \times V \quad (2)$$

Where  $q_m$  (mg g<sup>-1</sup>) is the adsorption capacity of the acetaminophen adsorbed on the adsorbent,  $C_0$  (mg L<sup>-1</sup>) is the initial concentration of acetaminophen,  $C_t$  (mg L<sup>-1</sup>) is the final concentration of the remaining acetaminophen at time  $t$ ,  $m$  (mg) is the mass of the ACNFs used, and  $V$  (L) is the volume of the acetaminophen solution.

### Characterization

The morphology of the nanofibers was examined by scanning electron microscopy (SEM) (JEOL JSM 6400, Tokyo, Japan). The samples were coated with a thin layer of gold and scanned at 2,500 ×, 5,000 ×, and 10,000 × magnifications. 20 readings of the nanofiber diameter were determined using ImageJ software to determine the average fiber diameter. The functional groups of the nanofibers were analyzed using an attenuated total reflectance Fourier transform infrared (ATR-FTIR) spectrometer (Perkin Elmer Spectrum RXI, Waltham, MA, USA) in the range 4000–280 cm<sup>-1</sup>.

## Results and Discussion

### PAN/SL nanofibers

Electrospun PAN/SL nanofibers were prepared by blending different PAN:SL ratios to determine the optimal structure and morphology required for preparing

ACNFs. The ratios of PAN to SL were 9:1, 8:2, 7:3, 6:4, and 5:5, as shown in Figure 1. The average diameter of the PAN/SL nanofibers with a 9:1 ratio was  $718 \pm 44$  nm, 8:2 ratio was  $698 \pm 47$  nm, 7:3 ratio was  $505 \pm 53$  nm, 6:4 ratio was  $472 \pm 68$  nm, and 5:5 ratio was  $455 \pm 41$  nm. The SEM micrographs showed the formation of small beads on the surface of the nanofibers for the 9:1, 7:3, 6:4, and 5:5 PAN/SL fibers. Meanwhile, the uniform and mostly bead-free fibers were obtained using the 8:2 PAN/SL ratio. At a low PAN composition, the size of the

beads is enlarged but with a thinner average fiber diameter, transforming the shape from spindle-like to a spherical bead structure. Thus, the 8:2 PAN/SL ratio was chosen for synthesizing activated carbon nanofibers (ACNFs). The relationship between the PAN/SL ratio and diameter of the electrospun PAN/SL nanofibers is shown in Figure 2. The average nanofiber diameter decreased gradually when lower amounts of lignin were used. The average fiber diameter was reduced to below 500 nm when the SL composition was above 30%.

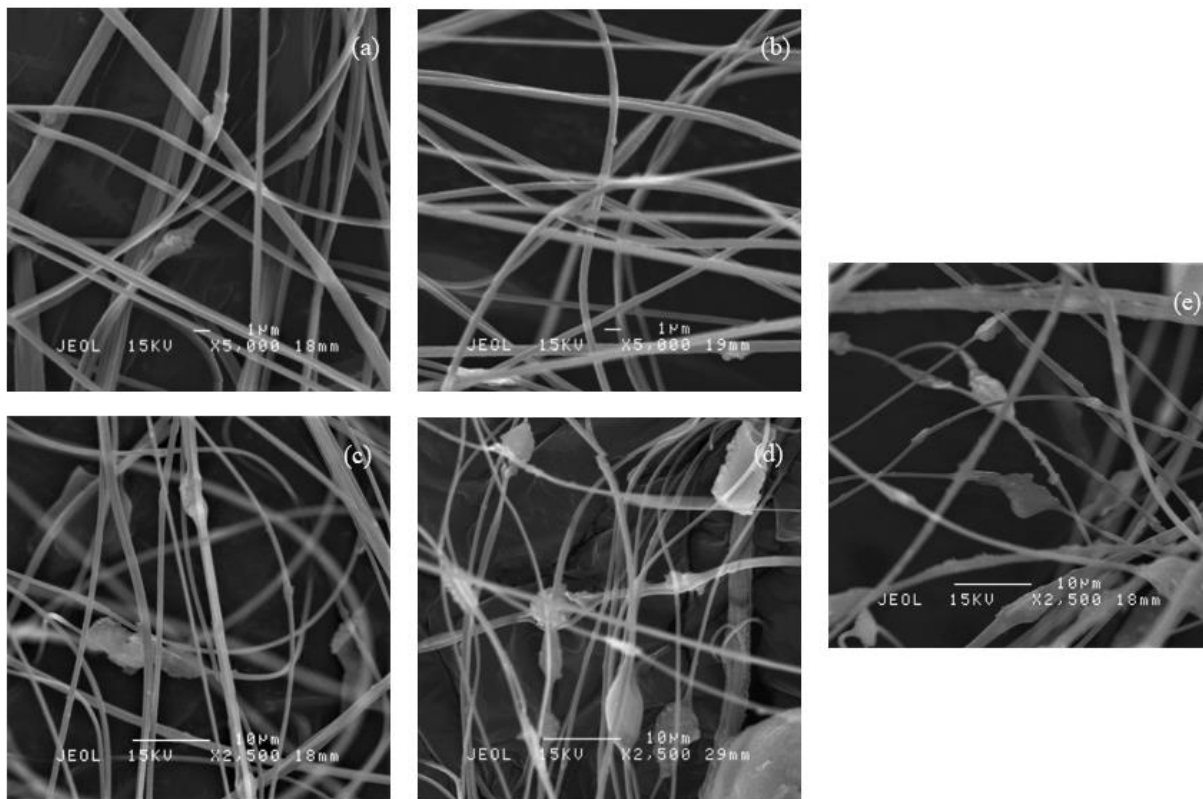


Figure 1. SEM micrographs of PAN/SL nanofibers: (a) 9:1, (b) 8:2, (c) 7:3, (d) 6:4, and (e) 5:5

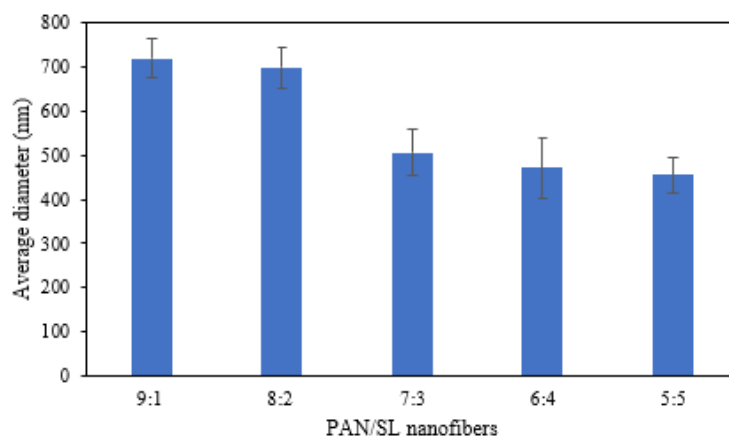


Figure 2. Effect of different PAN/SL ratios on the average diameter of fibers

Figure 3 demonstrates the ATR-FTIR spectra of sago lignin (SL) and the fibers obtained at different PAN/SL ratios. Sago lignin showed a broad band at approximately  $3360\text{ cm}^{-1}$ , attributed to the hydroxyl groups in phenolic and aliphatic structures, and a peak at  $2921\text{ cm}^{-1}$ , attributed to the aliphatic C–H stretching of the methoxy group of lignin [22]. A typical band at  $1632\text{ cm}^{-1}$  originated from the skeletal and stretching vibrations of the C=C bond in the benzene rings. The absorption peak at  $1453\text{ cm}^{-1}$  originated from the vibration C–C in the aromatic ring. A sharp peak appeared at  $1056\text{ cm}^{-1}$  corresponding to the C–O bond of the ether linkage of the guaiacyl units in sago lignin [23]. The FTIR spectra were interpreted based on the chemical structures of PAN and sago lignin. Based on the spectra, it presents mainly three stretching peaks, the first located around  $3300\text{ cm}^{-1}$  and  $2921\text{ cm}^{-1}$ , which can be attributed to the C–H stretching of PAN and methyl groups of sago lignin, and the second located around  $1450\text{ cm}^{-1}$ , assigned to the aromatic ring stretching of C–C. The third stretching band appeared at approximately  $1600\text{ cm}^{-1}$  and  $1630\text{ cm}^{-1}$ , corresponding to C=C in the benzene ring. Moreover, the absorption band around  $1060\text{ cm}^{-1}$  was attributed to the C–O bond of the ether and phenolic groups in sago lignin [24].

#### PAN/SL nanofibers after stabilization

PAN/SL (8:2) nanofibers were used for stabilization. The nanofibers underwent dehydrogenation and intracyclization reactions during the thermal treatment, resulting in a thermally stable ladder-like polymeric structure [25]. The stabilization of nanofibers is very

important for maintaining the fibrous structure and preventing it from melting and fusing during high-temperature carbonization [26]. Figure 4 shows the ATR-FTIR spectrum of PAN/SL 8:2 nanofiber as spun and stabilized. The functional groups remained unchanged after stabilization. The peaks at  $2935\text{ cm}^{-1}$  and  $1674\text{ cm}^{-1}$  correspond to the C–H and C–C stretching of the aromatic ring, respectively. The peak at  $1088\text{ cm}^{-1}$  is related to the C–O bonds. After the stabilization process, the peaks at  $2935\text{ cm}^{-1}$ ,  $1620\text{ cm}^{-1}$ , and  $1450\text{ cm}^{-1}$  appeared less intense, which reflects the disappearance of linear structures resulting from the cyclization and dehydrogenation reactions. These results imply that the nanofibers underwent cyclization during stabilization [27]. A new peak appeared at approximately  $1490\text{ cm}^{-1}$ , which can be attributed to the overlapping of different vibration modes, presumably from C=C, C=N, C=O, and N–H [28].

Figure 5 illustrates the SEM images of the stabilized 8:2 PAN/SL nanofibers. No significant changes were observed in the morphology of the nanofibers after the heat treatment at  $235\text{ }^{\circ}\text{C}$  for 1 h. However, the average diameter of the nanofibers decreased from  $698 \pm 47$  to  $389 \pm 57\text{ nm}$ . The physical shrinkage occurred during stabilization due to the release of inner physical stress, while the cyclization process caused the chemical shrinkage [29]. The color of the nanofibers also changed from white to dark brown after stabilization, which might be due to the formation of a ladder structure in the nanofibers [30].

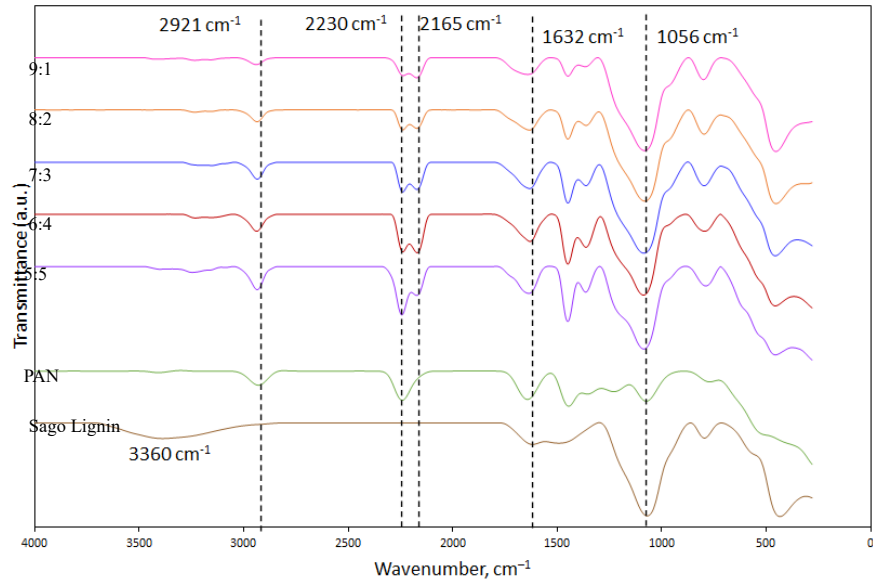


Figure 3. ATR-FTIR spectra of sago lignin, PAN, and PAN/SL nanofibers at different PAN to SL ratios

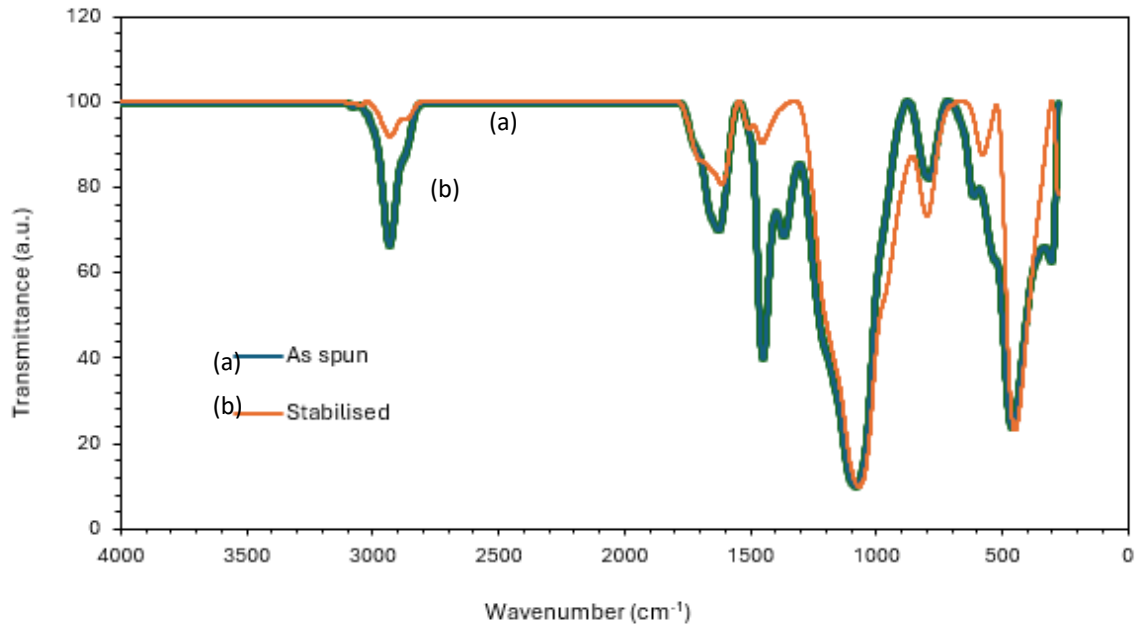


Figure 4. ATR-FTIR spectrum of PAN/SL (8:2) fibers as spun and after stabilization

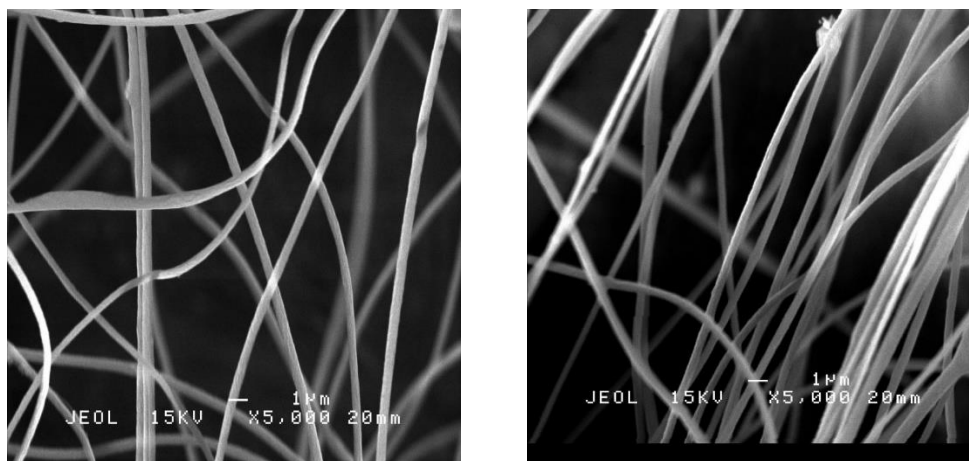


Figure 5. SEM images of stabilized 8:2 PAN/SL nanofibers

### PAN/SL CNFs and ACNFs

Carbonization was the second heat treatment of the nanofibers, which transformed the PAN/SL into carbon nanofibers. The PAN/SL-stabilized nanofibers were subjected to carbonization at 1000 °C for 1 h under a nitrogen atmosphere. During the carbonization step, inert gas flow was used to prevent polymer chain decomposition [31]. Carbonization removes non-carbon atoms such as hydrogen, nitrogen, and oxygen [30]. The inert gas flow dilutes the toxic gas and prevents the entry of atmospheric air, which can cause the combustion of lignin-based nanofibers [32]. PAN/SL CNFs were activated at 900 °C under a N<sub>2</sub> atmosphere for 2 h.

Activated carbon can be synthesized using various activation agents and is widely applied in wastewater treatment, energy storage devices, and other fields [33].

KOH activation is one of the most widely used chemical activations for generating porous structures with high surface areas and oxygenated functional groups [34]. The effect of KOH activation on the functional groups of PAN/SL ACNFs was determined using FTIR spectroscopy. Figure 6 shows the IR spectra of PAN/SL ACNFs and CNFs. The absorption peaks of the PAN/SL CNFs and ACNFs are listed in Table 1. For the PAN/SL ACNFs, the intensities of the absorption bands at 1653 cm<sup>-1</sup>, 1514 cm<sup>-1</sup>, and 1352 cm<sup>-1</sup> increased significantly compared to those of the PAN/SL CNFs after KOH activation. In addition, a sharp peak appeared at 1060 cm<sup>-1</sup>, which corresponds to the C–O functional group in the ACNFs after KOH activation. This indicates that the number of oxygen-containing functional groups in the ACNFs increased after activation.

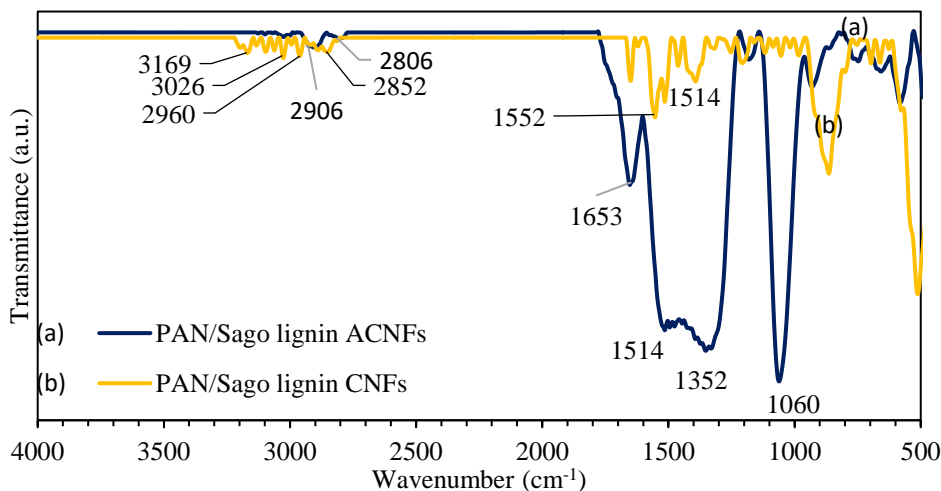


Figure 6. FTIR spectra of PAN/SL CNFs and PAN/SL ACNFs

Table 1. Functional groups of PAN/SL CNFs and PAN/SL ACNFs

PAN/SL CNFs		PAN/SL ACNFs	
Wavenumber (cm <sup>-1</sup> )	Bond	Wavenumber (cm <sup>-1</sup> )	Bond
3169	C-H stretching of aliphatic carbon	2906	C-H stretching
3026	C-H stretching of aromatic carbon	2806	C-H stretching
2960	C-H stretching aliphatic carbon	1653	C=C aromatic vibration
2852	C-H stretching of aromatic carbon	1514	C=C aromatic vibration
1552	C=N stretching	1060	C-O stretching
1514	C=C aromatic vibration		

**The comparison of morphology between PAN/SL CNFs and ACNFs: PAN/SL CNFs**

SEM images of the PAN/SL CNFs are shown in Figure 7. From these images, it can be deduced that the structure of the nanofibers remained intact after carbonization. The average fiber diameter (Figure 8) decreased slightly from  $389 \pm 57$  to  $302 \pm 42$  nm. This is due to the reaction during the carbonization process, which eliminates non-carbon elements. The average diameter was further reduced after carbonization compared to the stabilized PAN/SL nanofibers. Dehydrogenation, deoxygenation,

and denitrogenation of the precursor during decarbonization form a more compact structure [35-36]. At the beginning of the carbonization process, the stabilized nanofibers were cross-linked, and the cyclized structure was linked in the lateral direction by denitrogenation and dehydration. Cross-linking removes HCN and NH<sub>3</sub>, leading to the formation of carbon basal planes in the nanofibers. The carbon basal plane grew in the structure during carbonization, releasing N<sub>2</sub> through denitrogenation [37].

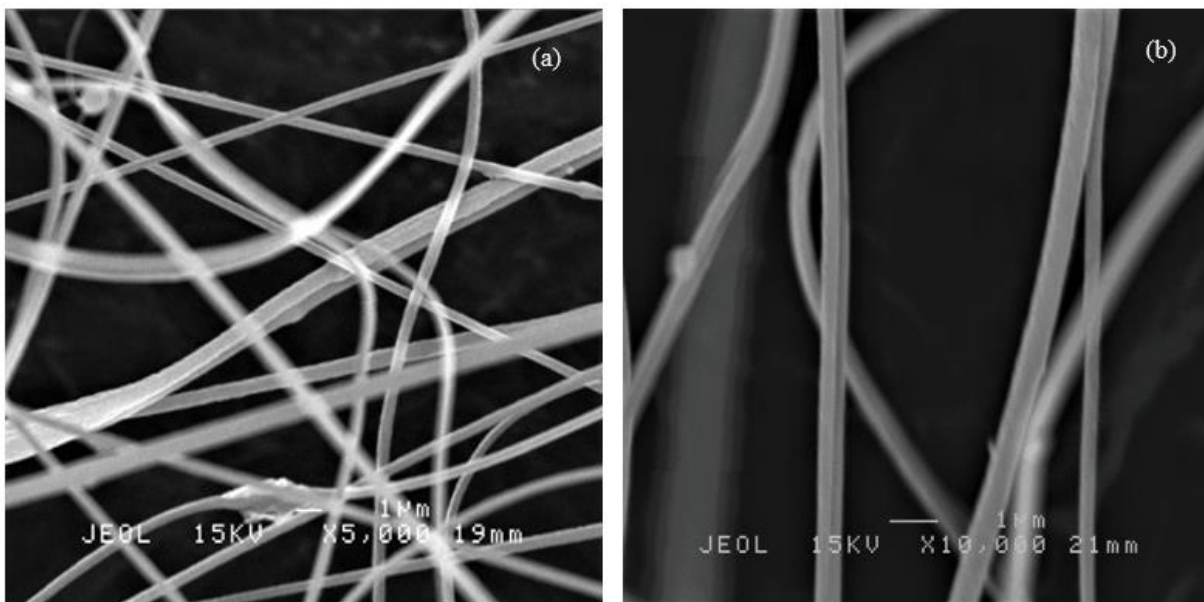


Figure 7. SEM images of PAN/SL CNFs at (a)  $\times 5,000$  and (b)  $\times 10,000$  magnification

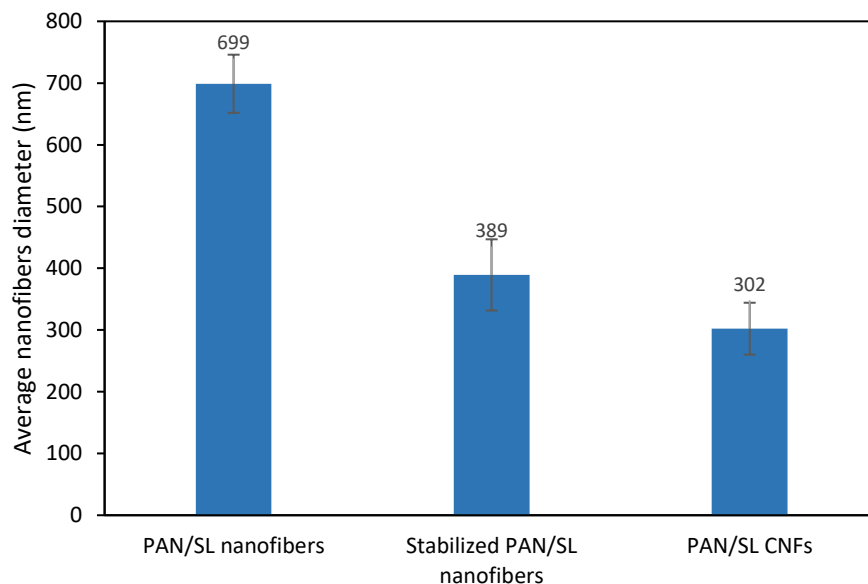
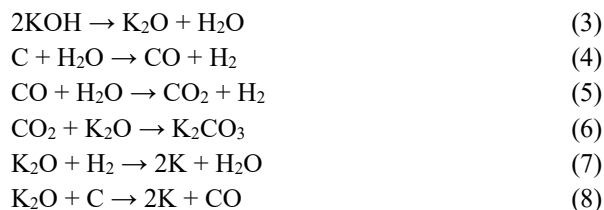


Figure 8. Comparison of average fiber diameters of PAN/SL nanofibers, stabilized PAN/SL nanofibers, and PAN/SL CNFs

#### PAN/SLACNFs

Figure 9 shows the SEM images and average fiber diameters of the PAN/SL ACNFs. The fiber diameter decreased from  $302 \pm 42$  to  $230 \pm 27$  nm. In this study, carbon nanofibers were activated with KOH under a nitrogen atmosphere at  $900\text{ }^{\circ}\text{C}$ . KOH was mainly used to create small micropores in the carbon skeleton. The activation mechanism was proposed to follow the release of K ions when reacted with carbon. The K ions were inserted into the carbon lattice, accompanied by carbon oxidation and activation with in situ  $\text{CO}_2$  or CO formation during high-temperature treatments [38]. KOH activation resulted in the following redox reactions:



According to this reaction mechanism, carbon and nitrogen in the activated carbon lattice were oxidized by KOH, and oxygen functional groups were introduced, consequently increasing the oxygen content [39].

#### Adsorption of acetaminophen: Effect of initial concentration of acetaminophen

Figure 10 shows the adsorption capacities of the PAN/SL CNFs and PAN/SL ACNFs at initial concentrations ranging from 25 to 100 mg/L. The acetaminophen adsorption on PAN/SL CNFs increased slightly from 25 mg/L to the maximum sorption of 9.08 mg/g at 100 mg/L of acetaminophen. For the PAN/SL ACNFs, the adsorption capacity increased from 12.79 to 46.23 mg/g as the acetaminophen concentration increased from 25 to 100 mg/L, respectively. Acetaminophen molecules can bind to active sites at low concentrations because of attractive forces such as electrostatic and van der Waals forces. Nevertheless, adsorbate–adsorbent interactions are inhibited by the mass transfer resistance between the aqueous and solid phases. More adsorbate molecules were adsorbed at higher concentrations onto the PAN/SL ACNFs surface. Therefore, there was a difference between the initial and final adsorbate concentrations; thus, the adsorption capacity increased [40]. In comparison, the adsorption capacity of PAN/SL ACNFs was three times higher than PAN/SL CNFs. This phenomenon can be explained by the PAN/SL ACNFs having a higher number of functional groups than the PAN/SL CNFs, hence, more adsorption sites were available for adsorption (as confirmed by the FTIR spectra in Figure 6. Figure 11 shows that the percentage removal of acetaminophen decreased from 93.61 to

84.60% with increasing acetaminophen concentrations. A fixed adsorbent dosage provided limited active sites for acetaminophen adsorption as the acetaminophen concentration increased. Thus, more acetaminophen molecules remained in the solution than those adsorbed

by PAN/SL ACNFs [40]. PAN/SL CNFs show very low adsorption capacity and percentage of removal. The following optimization parameters were focused only on the PAN/SL ACNFs.

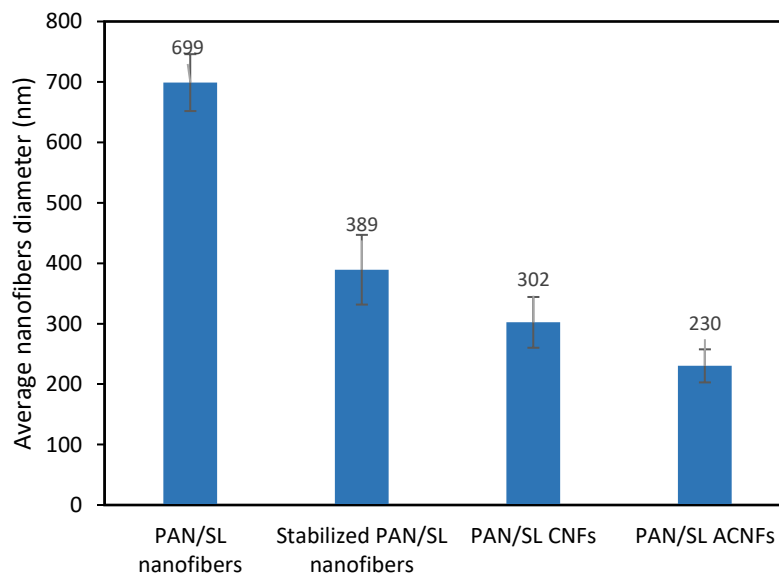
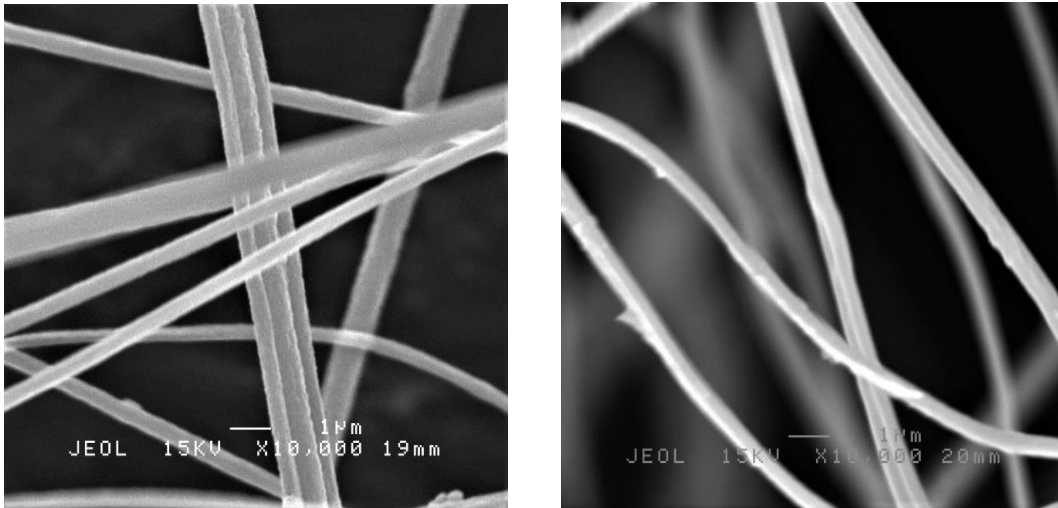


Figure 9. SEM images of PAN/SL ACNFs and the average fiber diameters of PAN/SL (8:2) nanofibers, stabilized PAN/SL nanofibers, PAN/SL CNFs, and PAN/SL ACNFs

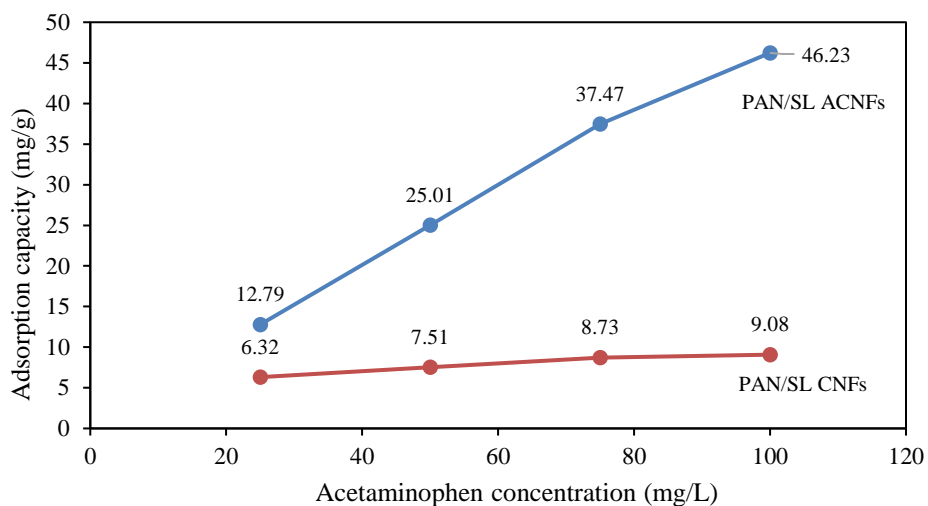


Figure 10. Effect of initial concentration on acetaminophen adsorption by PAN/SL CNFs and PAN/SL ACNFs. [Condition: adsorbent dosage = 0.05 g, contact time = 60 mins, pH 7]

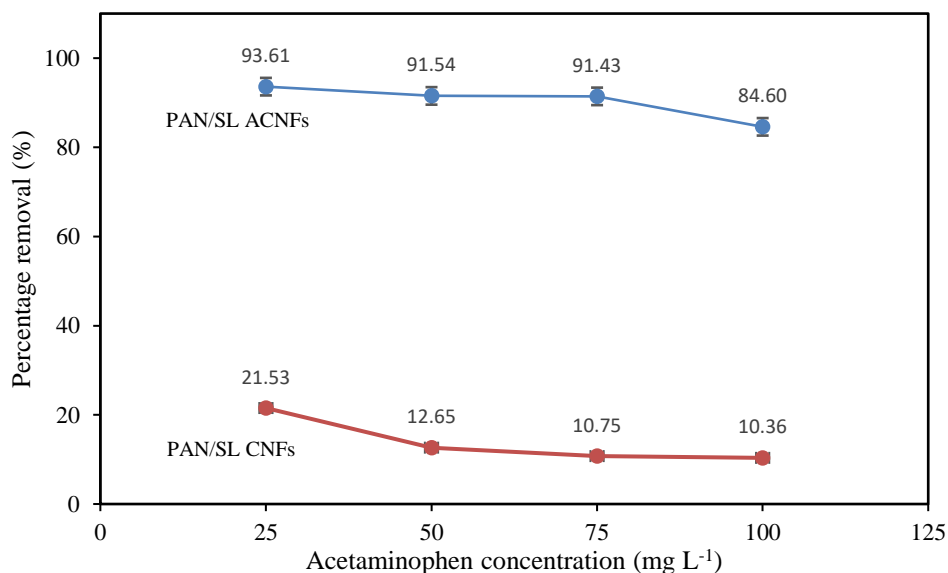


Figure 11. The percentage removal of acetaminophen by PAN/SL CNFs and PAN/SL ACNFs. [Condition: adsorbent dosage = 0.05 g, contact time = 60 mins, pH 7]

#### Effect of contact time

The effect of the contact time on acetaminophen adsorption showed a steady increase in removal from 0 to 50 min (Figure 12). This was due to the large number of vacant sites available on the surface of the adsorbent. As the adsorption progressed, more active sites were occupied by the adsorbate molecules, increasing the

resistance of acetaminophen to diffuse deeper into the adsorbent. The optimum time for the maximum removal of acetaminophen was 60 min because the adsorption sites on the PAN/SL ACNFs were fully saturated. After 60 min, no significant changes in the ions were adsorbed because equilibrium was achieved. As time proceeds, the oscillation between acetaminophen ions and PAN/SL

ACNFs particles is enhanced, which increases the concentration gradient and rate of mass transfer. Generally, these forces enhance acetaminophen uptake by PAN/SL ACNFs [41]. Therefore, the optimum contact time for the highest percentage of acetaminophen removal was 60 min.

#### Effect of adsorbent dosage

Figure 13 shows the percentage removal and adsorption capacity of different PAN/SL ACNFs dosages. The percentage removal of acetaminophen was slightly high (> 50%) at a low amount of adsorbent and steadily increased until the adsorbent dosage was 0.1 g to give 89.48 % removal. A high adsorbent dosage provides more active sites for adsorption, thereby improving the removal efficiency at the initial stage of the process. However, according to Wong et al. (2018) [42], the removal percentage was slightly reduced when the dosage was increased. This is due to the partial aggregation or overlapping of active sites, directly resulting in decreased active sites. Several adsorption studies have reported that increasing the adsorbent dosage increases the removal percentage to the optimum point, where the value becomes stagnant and occasionally decreases [43]. Hence, the optimum adsorbent dosage was 0.1 g, considering the percentage removal and the  $q$  value.

#### Effect of pH

The effect of pH on the adsorption of acetaminophen was studied in the pH range of 3-11. The pH changes the adsorbent surface charge and the possible ionic form of the adsorbate species [42]. Figure 14 illustrates the effect of the pH on the percentage removal of acetaminophen. The removal percentage slightly increased at pH 3-7. However, from pH 9 to 11, the percentage of removal decreased. The optimum removal percentage of 89.48% was obtained at a pH of 7. This is related to the interactions between the functional groups on the adsorbent surface and acetaminophen molecules. Acetaminophen is a weak acid ( $pK_a$  9.38) that partially dissociates in water to form anions. The compound remained predominantly a neutral species in solution at

pH < 9.38. When the pH exceeded 9.38, the acetaminophen dissociation increased, subsequently enhancing the abundance of negatively charged species in the solution. Therefore, the reduction in the removal percentage at high pH is due to the electrostatic repulsion between the anionic species of acetaminophen and the surface of the PAN/SL ACNFs [42]. In addition, Dutta et al. (2015) [44] stated that competition between acetaminophen and hydroxide ions occurred at a higher pH, reducing the removal percentage.

The adsorption process of polar aromatic pollutants such as acetaminophen in aqueous solution onto porous carbon-based materials such as PAN/SL ACNF can be associated with several possible interaction mechanisms, including  $\pi$ - $\pi$  interactions, electrostatic attraction, H-bonding, van der Waals forces, ion exchange, and pore-filling [45]. Previous studies proposed that H-bonding interactions are the primary mechanism for the adsorption of aromatic contaminants in water by carbon-based adsorbents [46,47]. ACNF contains various polar functional groups, such as carboxylic acid, -COOH, and hydroxyl groups, -OH, which can interact with the -OH and -NH moieties in the acetaminophen compound structure through H-bond formation [48]. The adsorption of acetaminophen on the PAN/SL ACNF surface can also be formed through  $\pi$ - $\pi$  interactions between the  $\pi$  electrons of the conjugated aromatic moieties in ACNF and the  $\pi$  electrons in the benzene ring of the acetaminophen molecule [46] and the  $n$ - $\pi$  electron interaction between the lone pair of electrons on the oxygen of the carbonyl groups on the surface of ACNF and the benzene ring of acetaminophen [48]. However, the main adsorption mechanism is often strongly reliant on three main elements: first, the environment of the adsorption process, including the pH of the solution, adsorbent dosage, temperature, and initial adsorbate concentration. Second, adsorbate properties, such as  $pK_a$  and electron distribution, and third, adsorbent characteristics, such as surface area, pore size distribution, and surface functional groups [45].

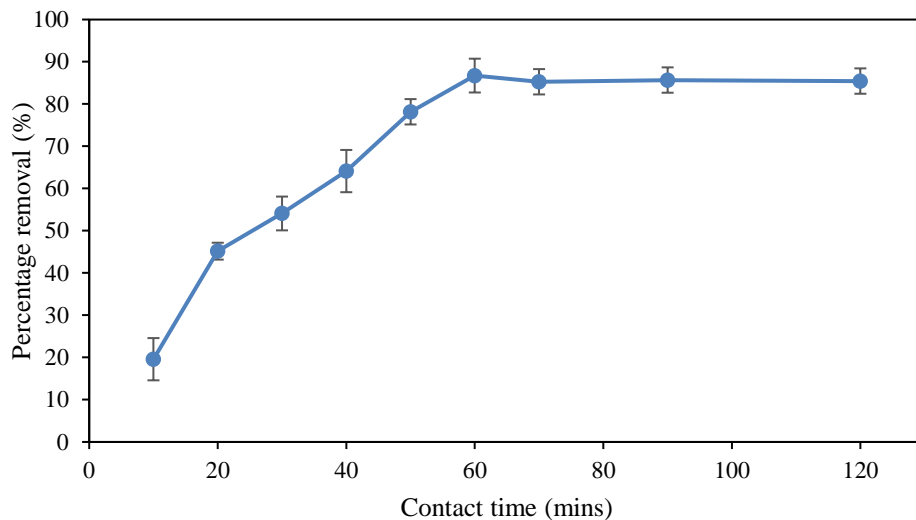


Figure 12. Effect of contact time on acetaminophen adsorption by the PAN/SL ACNFs. [Condition: Initial concentration of acetaminophen = 100 mg/L, adsorbent dosage = 0.05 g, pH 7]

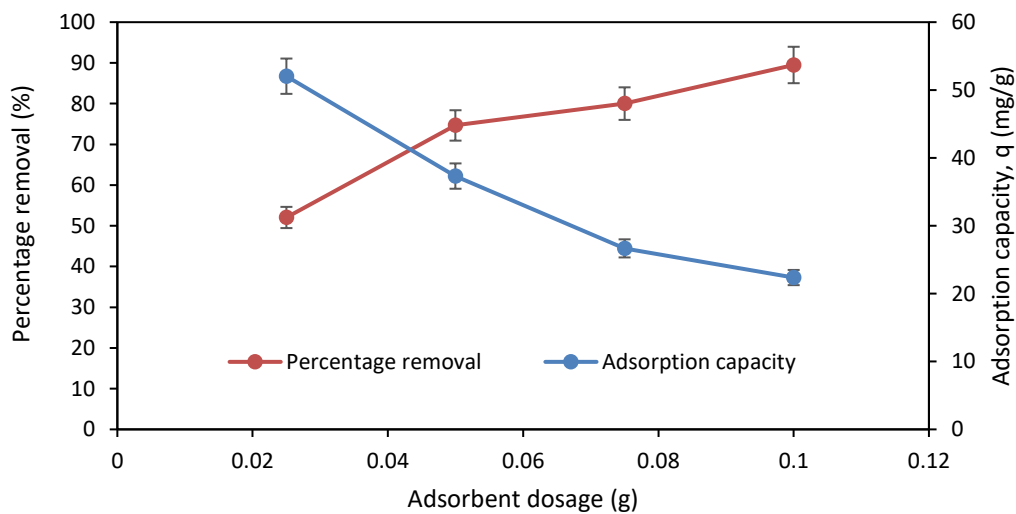


Figure 13. Effect of adsorbent dosage on acetaminophen adsorption by the PAN/SL ACNFs. [Condition: Initial concentration of acetaminophen = 100 mg/L, contact time = 60 mins, pH 7]

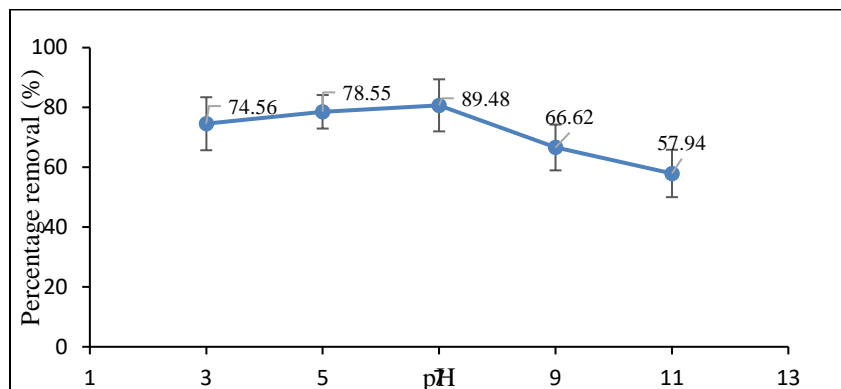


Figure 14. Effect of pH on acetaminophen adsorption by the PAN/SL ACNFs. [Condition: initial concentration of acetaminophen = 100 mg/L, contact time = 60 mins, adsorbent dosage = 0.1 g]

### Conclusion

Sago lignin was blended with PAN at different ratios to produce PAN/SL nanofibers via electrospinning. Variations in the PAN/SL ratios showed that the optimum 8:2 PAN/SL nanofibers had a uniform morphology with no apparent bead structures and were chosen for further thermal treatments to synthesize PAN/SL CNFs and PAN/SL ACNFs. The average fiber diameter decreased after the stabilization, carbonization, and activation processes. The PAN/SL CNFs were activated using KOH to produce PAN/SL ACNFs, which were used for the adsorption of acetaminophen from aqueous water. The adsorption of acetaminophen on the PAN/SL ACNF was evaluated based on four parameters: the effect of the initial concentration of acetaminophen, contact time, adsorbent dosage, and pH. The adsorption capacity and removal percentage of the PAN/SL CNFs were also examined for the initial concentration parameters. The adsorption capacity of the PAN/SL ACNFs was approximately three times higher than that of PAN/SL CNFs. The adsorption results showed that the absorption behavior of the PAN/SL ACNFs was independent at pH 3-9 with no significant changes in the range. The optimum parameters for acetaminophen were found to be an initial concentration of 25 mg/L, an adsorbent dose of 0.1 g, and a reaction time of 60 min.

### Acknowledgement

The authors are grateful for the financial support from the Ministry of Education Malaysia (FRGS/1/2019/STG01/UPM/02/7). The authors also greatly acknowledge the Nuclear Agency Malaysia for providing the sago waste.

### References

1. Qadir, M., Drechsel, P., Jiménez Cisneros, B., Kim, Y., Pramanik, A., Mehta, P., and Olaniyan, O. (202). Global and regional potential of wastewater as a water, nutrient and energy source. *Nature Resource Forum*, 44(1), 40-51.
2. Geissen, V., Mol, H., Klumpp, E., Umlauf, G., Nadal, M., van der Ploeg, M., ... and Ritsema, C. J. (2015). Emerging pollutants in the environment: a challenge for water resource management. *International Soil and Water Conservation Research*, 3(1): 57-65.
3. Wood, D. M., English, E., Butt, S., Ovaska, H., Garnham, F., and Dargan, P. I. (2010). Patient knowledge of the paracetamol content of over-the-counter (OTC) analgesics, cough/cold remedies and prescription medications. *Emergency Medicine Journal*, 27(11): 829-833.
4. Parry, M. J., Isoniemi, H., Koivusalo, A. M., and Hoppu, K. (2018). Increased acetaminophen related calls to Finnish PIC better reflect acetaminophen sales than serious poisonings. *Clinical toxicology*, 56(3): 209-215.
5. Carvalho, A. P., Mestre, A. S., Haro, M., and Ania, C. O. (2012). Advanced methods for the removal of acetaminophen from water. *Acetaminophen: Properties, clinical uses and adverse effects: Nova Science Publishers*, 57-105.
6. Vidovix, T. B., Januário, E. F. D., Bergamasco, R., and Vieira, A. M. S. (2022). Evaluation of agro-industrial residue functionalized with iron oxide magnetic nanoparticles for chloroquine removal from contaminated water. *Materials Letters*, 326: 132915.

7. Ye, C., Pan, Z., and Shen, Y. (2022). Facile Conversion of polystyrene waste into an efficient sorbent for water purification. *Polymers*, 14(21): 4477.
8. Nordin, N. A., Abdul Rahman, N., and Abdullah, A. H. (2020). Effective removal of Pb(II) ions by electrospun PAN/Sago lignin-based activated carbon nanofibers. *Molecules*, 25(13): 3081.
9. Jjagwe, J., Olupot, P. W., Menya, E., and Kalibbala, H. M. (2021). Synthesis and application of granular activated carbon from biomass waste materials for water treatment: A review. *Journal of Bioresources and Bioproducts*, 6(4): 292-322.
10. Terzyk, A. P., Pacholczyk, A., Wiśniewski, M., and Gauden, P. A. (2012). Enhanced adsorption of paracetamol on closed carbon nanotubes by formation of nanoaggregates: Carbon nanotubes as potential materials in hot-melt drug deposition-experiment and simulation. *Journal of Colloid and Interface Science*, 376(1): 209-216.
11. Zhang, W., Yang, P., Li, X., Zhu, Z., Chen, M., and Zhou, X. (2019). Electrospun lignin-based composite nanofiber membrane as high-performance absorbent for water purification. *International Journal of Biological Macromolecules*, 141: 747-755.
12. Kolluru, S. S., Agarwal, S., Sireesha, S., Sreedhar, I., and Kale, S. R. (2021). Heavy metal removal from wastewater using nanomaterials-process and engineering aspects. *Process Safety and Environmental Protection*, 150: 323-355.
13. Xu, T. C., Han, D. H., Zhu, Y. M., Duan, G. G., Liu, K. M., and Hou, H. Q. (2021). High strength electrospun single copolyacrylonitrile (coPAN) nanofibers with improved molecular orientation by drawing. *Chinese Journal of Polymer Science*, 39: 174-180.
14. Ali, A. B., Slawig, D., Schlosser, A., Koch, J., Bigall, N. C., Renz, F., ... and Sindelar, R. (2021). Polyacrylonitrile (PAN) based electrospun carbon nanofibers (ECNFs): Probing the synergistic effects of creep assisted stabilization and CNTs addition on graphitization and low dimensional electrical transport. *Carbon*, 172: 283-295.
15. Robledo-Peralta, A., Torres-Castañón, L. A., Rodríguez-Beltrán, R. I., and Reynoso-Cuevas, L. (2022). Lignocellulosic biomass as sorbent for fluoride removal in drinking water. *Polymers*, 14(23): 5219.
16. Luo, J., and Liu, T. L. (2023). Electrochemical valorization of lignin: Status, challenges, and prospects. *Journal of Bioresources and Bioproducts*, 8(1): 1-14.
17. Duval, A., and Lawoko, M. (2014). A review on lignin-based polymeric, micro-and nano-structured materials. *Reactive and Functional Polymers*, 85: 78-96.
18. Kumar, M., Hietala, M., and Oksman, K. (2019). Lignin-based electrospun carbon nanofibers. *Frontiers in Materials*, 6: 62.
19. Obst, J. R., and Kirk, T. K. (1988). Isolation of lignin. In *Methods in enzymology* (Vol. 161, pp. 3-12). Academic Press.
20. Mistar, E. M., Alfatah, T., and Supardan, M. D. (2020). Synthesis and characterization of activated carbon from *Bambusa vulgaris striata* using two-step KOH activation. *Journal of Materials Research and Technology*, 9(3): 6278-6286.
21. Wang, Y., Liu, W., Zhang, L., and Hou, Q. (2019). Characterization and comparison of lignin derived from corncob residues to better understand its potential applications. *International Journal of Biological Macromolecules*, 134: 20-27.
22. Zhuang, J., Li, M., Pu, Y., Ragauskas, A. J., & Yoo, C. G. (2020). Observation of potential contaminants in processed biomass using fourier transform infrared spectroscopy. *Applied Sciences*, 10(12): 4345.
23. Ramasubramanian, G. (2013). Influence of Lignin modification on PAN-Lignin copolymers as potential carbon fiber precursors. Dissertation thesis Iowa state University.
24. Wu, M., Wang, Q., Li, K., Wu, Y., & Liu, H. (2012). Optimization of stabilization conditions for electrospun polyacrylonitrile nanofibers. *Polymer Degradation and Stability*, 97(8): 1511-1519.
25. Zhang, B., Kang, F., Tarascon, J. M., and Kim, J. K. (2016). Recent advances in electrospun carbon nanofibers and their application in electrochemical energy storage. *Progress in Materials Science*, 76: 319-380.
26. Duan, Y., Gu, T. J., Jiang, C. L., Yuan, R. S., Zhang, H. F., Hou, H. J., ... and Kong, W. (2012). A novel disulfide-stabilized single-chain variable antibody fragment against rabies virus G protein with enhanced in vivo neutralizing potency. *Molecular Immunology*, 51(2): 188-196.

27. Lee, Y. J., Kim, J. H., Kim, J. S., Lee, D. B., Lee, J. C., Chung, Y. J., and Lim, Y. S. (2004). Fabrication of activated carbon fibers from stabilized PAN-based fibers by KOH. In *Materials Science Forum* (Vol. 449, pp. 217-220). Trans Tech Publications Ltd.
28. Xiao, S., Lv, H., Tong, Y., Xu, L., and Chen, B. (2011). Thermal behavior and kinetics during the stabilization of polyacrylonitrile precursor in inert gas. *Journal of Applied Polymer Science*, 122(1): 480-488.
29. Rahaman, M. S. A., Ismail, A. F., and Mustafa, A. (2007). A review of heat treatment on polyacrylonitrile fiber. *Polymer degradation and Stability*, 92(8): 1421-1432.
30. Maradur, S. P., Kim, C. H., Kim, S. Y., Kim, B. H., Kim, W. C., and Yang, K. S. (2012). Preparation of carbon fibers from a lignin copolymer with polyacrylonitrile. *Synthetic Metals*, 162(5-6): 453-459.
31. Yan, B., Feng, L., Zheng, J., Zhang, Q., Jiang, S., Zhang, C., ... and He, S. (2022). High performance supercapacitors based on wood-derived thick carbon electrodes synthesized via green activation process. *Inorganic Chemistry Frontiers*, 9(23): 6108-6123.
32. Tadda, M. A., Ahsan, A., Shitu, A., ElSergany, M., Arunkumar, T., Jose, B., ... and Daud, N. N. (2016). A review on activated carbon: process, application and prospects. *Journal of Advanced Civil Engineering Practice and Research*, 2(1): 7-13.
33. Sing, K. S. W. (1967). *Adsorption, surface area, and porosity*. Academic press.
34. El-Merraoui, M., Aoshima, M., and Kaneko, K. (2000). Micropore size distribution of activated carbon fiber using the density functional theory and other methods. *Langmuir*, 16(9), 4300-4304.
35. Huang, X. (2009). Fabrication and properties of carbon fibers. *Materials*, 2(4): 2369-2403.
36. Wang, J., and Kaskel, S. (2012). KOH activation of carbon-based materials for energy storage. *Journal of Materials Chemistry*, 22(45): 23710-23725.
37. Zhou, M., Pu, F., Wang, Z., and Guan, S. (2014). Nitrogen-doped porous carbons through KOH activation with superior performance in supercapacitors. *Carbon*, 68: 185-194.
38. Wirasnita, R., Hadibarata, T., Yusoff, A. R. M., and Yusop, Z. (2014). Removal of bisphenol a from aqueous solution by activated carbon derived from oil palm empty fruit bunch. *Water, Air, & Soil Pollution*, 225: 1-12.
39. Al-Khateeb, L. A., Almotiry, S., and Salam, M. A. (2014). Adsorption of pharmaceutical pollutants onto graphene nanoplatelets. *Chemical Engineering Journal*, 248: 191-199.
40. Wong, S., Lee, Y., Ngadi, N., Inuwa, I. M., and Mohamed, N. B. (2018). Synthesis of activated carbon from spent tea leaves for aspirin removal. *Chinese Journal of Chemical Engineering*, 26(5): 1003-1011.
41. Kilic, M., Apaydin-Varol, E., and Pütün, A. E. (2011). Adsorptive removal of phenol from aqueous solutions on activated carbon prepared from tobacco residues: equilibrium, kinetics and thermodynamics. *Journal of Hazardous Materials*, 189(1-2): 397-403.
42. Dutta, M., Das, U., Mondal, S., Bhattacharya, S., Khatun, R., and Bagal, R. (2015). Adsorption of acetaminophen by using tea waste derived activated carbon. *International Journal of Environmental Sciences*, 6(2): 270-281.
43. Nguyen, D. T., Tran, H. N., Juang, R. S., Dat, N. D., Tomul, F., Ivanets, A., ... and Chao, H. P. (2020). Adsorption process and mechanism of acetaminophen onto commercial activated carbon. *Journal of Environmental Chemical Engineering*, 8(6): 104408.
44. Patel, M., Kumar, R., Pittman Jr, C. U., and Mohan, D. (2021). Ciprofloxacin and acetaminophen sorption onto banana peel biochars: Environmental and process parameter influences. *Environmental Research*, 201: 111218.
45. Liu, S., Pan, M., Feng, Z., Qin, Y., Wang, Y., Tan, L., and Sun, T. (2020). Ultra-high adsorption of tetracycline antibiotics on garlic skin-derived porous biomass carbon with high surface area. *New Journal of Chemistry*, 44(3): 1097-1106.
46. De Araújo, T. P., Quesada, H. B., Bergamasco, R., Vareschini, D. T., & De Barros, M. A. S. D. (2020). Activated hydrochar produced from brewer's spent grain and its application in the removal of acetaminophen. *Bioresource Technology*, 310: 1233